Contribution to the achievement of SDGs by Furukawa Electric Group

Contribution to R&D of Power Cable Systems by Applying Computer Simulation

Satoru Maruyama[*1], *Sakurako Tomii*[*1], *Yudai Tomita*[*1], *Yuki Matsumoto*[*2]

ABSTRACT In the Power Cable Division, we are focusing on the fields of submarine cables for renewable energy, direct current (DC) cables, and ultra-high voltage underground cables as the pillars of our efforts toward a decarbonized society and our Medium-term Management Plan 2022-2025 (2025 Mid-term Plan). The activities in order to increase the efficiency of product developments using scientific calculations are underway. This paper is described about the results obtained from the evaluation of steel wire armour loss in submarine cables, the evaluation of DC insulation materials based on quantum chemical calculations, and the simulation of the internal pressure when a ground fault occurs at cable terminations. It would be expected that these achievements will not only achieve our company's goals but will also contribute to technological developments on the power cable.

1. INTRODUCTION

The Power Cable Division has adopted submarine cables for renewable energy, DC cables, ultra-high voltage underground cables, etc. as the pillars of our 2025 Mid-term Plan, and is promoting related technology developments. In the past, as the design and development of power cables has focused on empirical methods, in which sample evaluations are followed by actual cable evaluations, the development period tended to be lengthened. Moreover, there is also a problem that the manufacturing of prototypes on the production line becomes a factor that inhibits the factory operating rate.

On the other hand, in industrial fields such as automobiles, design using computer aided engineering (CAE) is commonly performed. This not only reduces the time and the cost required for actual machine testing, but also reduces the dangers hidden in actual machine testing, which is considered to be a great advantage in terms of safety.

In the field of power cables, as voltages and capacities are increasing, experiments involving dangerous factors such as high voltages and large currents are essential for characterization. Therefore, it is considered that it is possible to reduce the risk associated with experiments by proceeding with a basic design based on CAE and only performing final verification at the actual cables. In addition, although alternating current (AC) power transmission is generally adopted, it is known that the materials themselves which make up the power cable generate losses due to AC magnetic fields, resulting in power transmission losses. The accurately estimation of these losses by applying the electromagnetic field is also effective for designing efficient transmission capacities.

Moreover, it is necessary to process at the atomic and the molecular levels which make up matters when considering material development. In the development of cable insulation materials, by incorporating the concept of quantum chemistry which has not been used much, it is possible to explain how insulation performance is efficiently expressed, and attempts are also being made to apply this to logical material design.

As described above, elucidation of physical phenomena through simulations based on CAE and scientific calculations is expected to become even more important for efficient development. Therefore, we are expanding their applications to design and develop to the power cable systems as well.

This paper presents the evaluation of material properties of DC insulating materials based on quantum chemical calculations, pressure simulation in cable termination when a ground fault occurs, and the optimization of steel wire armour losses in submarine cables as examples and shows the consistency between actual application examples and verification test results.

[*1] Cable System R&D Department, Power Cable Division
[*2] Cable System Engineering Department, Power Cable Division

2. CHEMICAL CALCULATIONS OF DC INSULATING MATERIALS

When a DC voltage is applied, a dielectric phenomenon peculiar to DC occurs in which electric charge accumulates (accumulation of space charge) inside the solid insulating materials used in cables and joints. Therefore, the development of materials which do not accumulate space charges has been being required. As a method for evaluating the accumulation of space charge, a method of experimentally measuring and evaluating is generally used. However, preparing evaluation sample materials and measuring all of them in the material development process poses the problem of cost and time.

On the other hand, the use of quantum chemical calculations is known as a method for predicting the movement of electric charges from the chemical structure of materials and evaluating their space charge characteristics[1]. This method enables the desk study of the space charge characteristics before measurement. This section introduces an example of an approach using quantum chemical calculations to evaluate the space charge characteristics of the main insulating material developed for applying to DC cable system.

A method for determining space charge characteristics from quantum chemical calculations will be explained using Figure 1. As an index for evaluating properties, the presence or absence and the size of the generation of an electric double layer and a trap level for each material are used and have a very large effect on the space charge characteristics.

Figure 1 shows an example of the energy potentials of the calculation model. From the energy potentials, the highest occupied molecular orbit (hereinafter referred to as HOMO), the lowest unoccupied molecular orbit (hereinafter referred to as LUMO), and the median value of the region (forbidden band) between HOMO and LUMO - called the Fermi level - were calculated. When a voltage is applied to an insulating material, the sample (S) is sandwiched between semiconducting (SC) or metallic (M) materials. The Fermi levels of semiconducting and metallic materials were set as fixed values, respectively, and the difference with the Fermi level of the sample was compared (Figure 1 (a): ΔE (SC-S), ΔE (M-S)). The larger the Fermi level difference, the easier it was for charges to be injected from the conductive material because a layer called an electric double layer was generated between the sample and the semiconducting/metal interface after the voltage application. In other words, the difficulty in forming an electric double layer leads to suppress space charge accumulation.

Furthermore, it is important to provide a mechanism called a trap level to prevent the free movement of charges when charges are injected into the sample. Depending on the molecular structure, trap levels (Figure 1 (b): Etrap (LUMO), Etrap (HOMO)) are generated where the charge density is locally concentrated. The deeper the trap level, the more difficult it is for the charge to transfer. From the quantum chemical calculation results of each material, the difficulty of the charge injection is determined from the Fermi level difference between the sample and the conductive material, and the difficulty of the charge transfer is determined from the depth of the trap level, thereby evaluating the space charge characteristics.

Here, the space charge characteristics about the following material were estimated from quantum chemical calculation results. One is the cross-linked polyethylene (XLPE) with a chemical structure of suppressing the charge accumulation which was developed for DC cable use (Hereafter, called DC-XLPE). The other is the ethylene propylene diene rubber (EPDM) used for the main insulation of the intermediate joint for DC cable system.

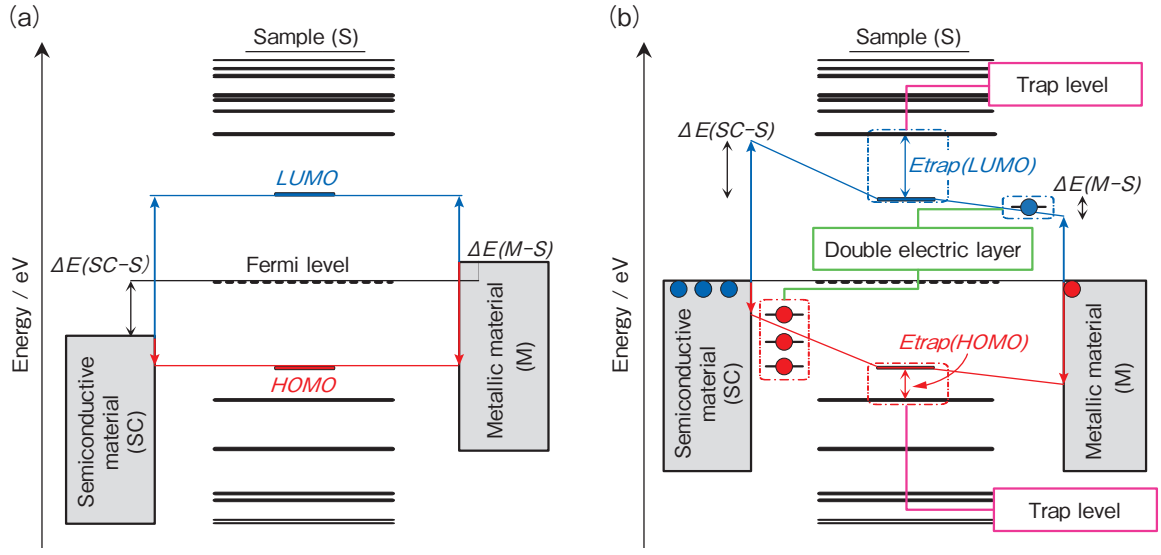

Figure 1 Characterization of space charge: (a) before voltage application (b) after voltage application.

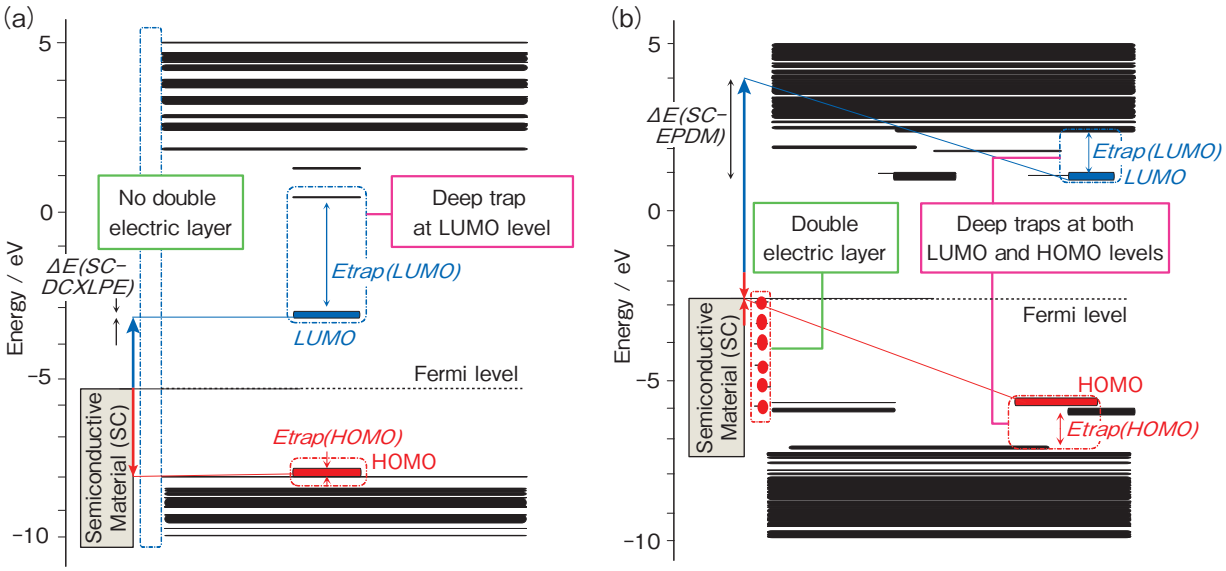

Figure 2 Energy potential of the DC-XLPE and the EPDM: (a) DC-XLPE (b) EPDM.

Figure 2 shows the energy potentials of the DC-XLPE and the EPDM. As shown in Figure 2 (a), the Fermi level difference between the DC-XLPE and the semiconducting material was very small, so an electric double layer was not generated and the charge injection was difficult to occur. Furthermore, there are few space charges accumulation because it had a structure of suppressing a charge transfer due to a generation of deep trap level in the LUMO level.

Next, as shown in the Figure 2 (b), it is found that EPDM is the material which the charge injection was easy to occur because the Fermi level difference between the EPDM and the semiconducting material is large, and a large number of electric double layers were formed. However, since relatively deep trap levels were generated at both the LUMO level and the HOMO level, the charge transfer was suppressed, which is considered to have a positive effect on the space charge characteristics.

Figure 3 shows the results of visualizing the charge density by mapping the charge density ratio in three dimensions. The DC-XLPE shown in Figure 3 (a) is characterized by a trap structure with a large negative charge. Deep traps were also confirmed from the energy potential, and it is considered that the structure that suppresses the charge accumulation was working effectively. In the case of the EPDM shown in Figure 3 (b), traps as deep as in the DC-XLPE were not generated, but a positive charge trap structure was partially formed. It is considered that a diene structure having a double bond has a good effect on the space charge characteristics.

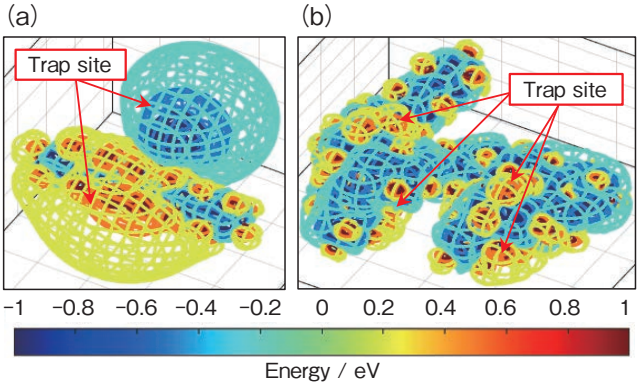

Figure 3 3D electrostatic potential of the DC-XLPE and the EPDM: (a) DC-XLPE (b) EPDM.

Quantum chemical calculations were used to evaluate the space charge characteristics of the insulating materials for cables and joints used in DC cable systems, and it was confirmed that they have good space charge characteristics. Pre-qualification (PQ) tests for DC 525 kV class cable system including cable, joints and other accessories using insulating materials described in this section have been performed, and they have been certified by third-party organizations[2), 3)].

Accordingly, it was confirmed that the insulating material developed were suitable for DC use.

As mentioned above, it is expected that these techniques by promoting for evaluations which combine quantum chemical calculations and space charge measurements would be contributed to accelerating the development speed in the future insulating material development process.

3. NUMERICAL ANALYSIS OF THE CABLE TERMINATION AT GROUND FAULT (ESTIMATION OF THE MAXIMUM PRESSURE)

As the capacity of power cables increases, there are concerns about increased damage in the event of an accident due to insulation breakdown, etc., and about the lengthening duration of the restoration work. In such a situation, as the terminations of power cables are designed to be filled with insulating oil, damage to peripheral equipment due to the damage of hollow insulators and environmental pollution damages due to the oil leakage can be expected if a ground fault occurs inside the termi-

nations. Therefore, there is a growing demand for a pressure relief mechanism at the termination to reduce damages in the event of an accident. Although a ground fault test is required for the performance verification in order to install the pressure relief mechanism, there is the problem of significant high cost because of safety and environmental measures in its test. Therefore, it is necessary to reproduce ground fault tests by numerical analysis and reduce the number of tests for design reviews. In here, focusing on the pressure generated when a ground fault occurs, we performed a ground fault equivalent test in order to establish an internal pressure estimation technology, set parameters based on the obtained results, and calculated changes in the internal pressure.

First, in order to understand the relationship between the ground fault energy and the generated pressure when a ground fault occurs, a ground fault equivalent test was performed using a scaled-down model to confirm the durability of the hollow insulator and verify the peak pressure.

In the ground fault equivalent test, explosives were used to generate pressure in order to simplify the relationship between the input energy and the generated pressure. The sample is a polymer composite hollow insulator used in a 66 kV class termination. As a pressure source, four cartridges containing explosives were connected to the bottom of the hollow insulator, the explosives were burned inside each, and the combustion gas was applied to the inside of the hollow insulator (Figure 4). The amount of explosive charged was calculated from the first peak value of the energy of the ground fault current when a ground fault occurred. Each cartridge was charged with 1.5 g of black powder and 5.0 g of smokeless powder and the four cartridges were ignited simultaneously. In this test, for safety reasons, the inside was filled with water instead of insulating oil. The internal pressure was measured with a pressure sensor connected to the upper part of the hollow insulator. Furthermore, in order to confirm the pressure transition and a maximum pressure value with the pressure relief mechanism, the samples with/without a rupture disk connected to the upper sealing plate were prepared. Here, a rupture disk used was the valve to burst at 0.6 MPa.

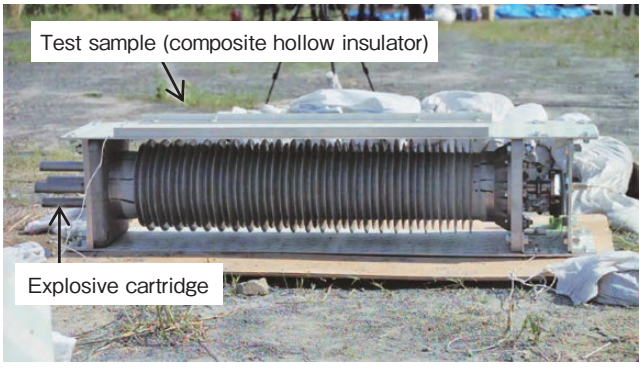

Figure 4 Sample for the ground fault equivalent test.

The test results are shown in Figure 5. The solid line is the pressure transition of the sample without a rupture disk, and the dashed line is the one with a rupture disk. In the sample without a rupture disk, the maximum pressure increased to 12.0 MPa, but no damage was observed in the hollow insulator and the sealing part, and the sealing performance was maintained. On the other hand, in the sample with a rupture disk, the rupture disk operated at the same time as the pressure increased and released the filled water. As a result, the maximum pressure was 9.0 MPa, the pressure rise after 15ms was very small, and the pressure release effect was confirmed after 15 ms. In addition, no damage was observed inside the sample and in the sealing part even in the sample with a rupture disk.

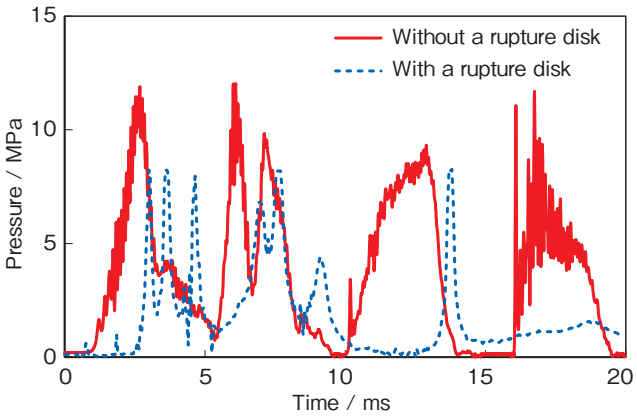

Figure 5 Measurement results of the internal pressure in the hollow insulator in the ground fault equivalence test.

This ground fault equivalent test was reproduced by numerical analysis using the finite element method. Since the ground fault phenomenon causes the pressure to change rapidly in a short time, it is necessary to solve the state equation which takes into account the impact of the shock wave. LS-DYNA was used as an analysis solver, and in this analysis, the pressure of the fluid inside the hollow insulator (p) was obtained using the Mie-Grüneisen state equation given by equation (1)[4].

$$p = \frac{\rho_0 c_0^2 \mu \left[1+\left(1-\frac{\Gamma_0}{2}\right)\mu\right]}{\left[1-(s-1)\mu\right]^2} + \Gamma_0 E \qquad (1)$$

Here, ρ_0 is the density, c_0 is the speed of sound, μ is the volume compressibility, s is the coefficient of the relational expression between the shock wave velocity and the material particle velocity, and Γ_0 is the Grüneisen constant. The values in Table 1 were set for each. In addition, E is the internal energy density of the material, and in the simulation analysis, the start time was the instant when the high-pressure gas flew into the hollow insulator, and the initial energy density was set so that the initial pressure inside the cartridge was 8.85 MPa, as shown in Table 1.

Table 1 Parameters for the simulation.

Symbol	Value	Unit
ρ_0	1.00×10^3	kg/m^3
c_0	1450	m/s
μ	1.00×10^{-9}	
s	1.79	
Γ_0	1.65	
E	22.1×10^6	J/m^3

The analysis result is shown in Figure 6. The solid line is the result without a rupture disk, and the dashed line is the result with a rupture disk. In the model without a rupture disk, the maximum pressure was 12.3 MPa, which almost matched the peak pressure in the equivalent test, and the second and subsequent pressure peaks occurred at almost the same timing. On the other hand, comparing between an equivalent test result and an analysis result with rapture disks, the former was indicated a peak pressure value of 9.0 MPa and the latter was 10.2 MPa. And the occurrence time on their pressure value is earlier in the analysis result. The cause of this difference is considered that the inflow timing of the pressurized gas from the four cartridges did not match up in the ground fault equivalent test.

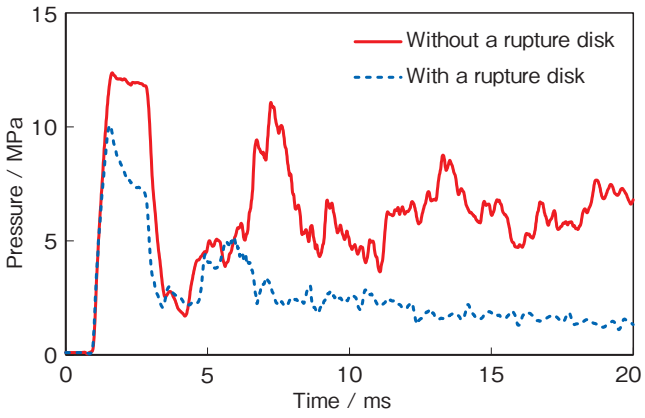

Figure 6 Simulation results of the interenal pressure in the hollow insulator.

It was confirmed that the analysis result qualitatively agreed with the test result by providing appropriate initial conditions when compared under the condition without a rupture disk. Therefore, the pressure estimation by numerical analysis is expected to become an effective mean when examining safety measures, etc. for ground fault tests if the accuracy of the analysis is improved.

Using this analysis method, the pressure during the ground fault test of a 500 kV-class termination was estimated. As shown in Figure 7, a model was created in which silicone oil was filled inside a hollow insulator with a length of 7.5 m and a diameter of 600 mm, and the Mie-Grüneisen state equation was calculated with the parameters in Table 2. It was assumed that the ground fault occurred directly under the stress cone inside the termination with a ground fault current of 30 kA for 0.25 seconds. The displacement of the central cable and the stress cone and the displacement of the hollow insulator surface were neglected. As analysis models, models with and without rupture disks were created. In the model with rupture disks, four rupture disks with the same area as in the ground fault equivalent test were set, and they were set to release the silicone oil inside when the pressure reached 0.6 MPa in each of the rupture disk position.

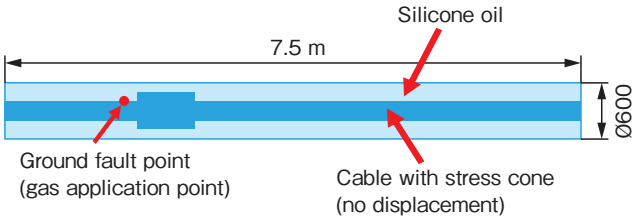

Figure 7 Schematic figure of the simulation model at ground fault in the 500 kV hollow insulator.

Table 2 Parameters for the simulation of the 500 kV termination.

Symbol	Value	Unit
ρ_0	9.85×10^2	kg/m^3
c_0	985	m/s
μ	9.85×10^{-8}	
s	0	
Γ_0	1.65	

Figure 8 shows the analysis result. The solid line is the analysis result without the rupture disk, and the dashed line is the one with rupture disks. In this analysis, since the ground fault gas continued to be supplied from the ground fault point, the pressure continued to rise under the condition without rupture disks to be estimated to reach 18 MPa or more at 0.25 seconds. On the other hand, under the condition with rupture disks, the pressure rise and the pressure reduction effect due to the release of the filling oil were balanced, and finally converged at 6.2 MPa. Considering the result of the above-mentioned ground fault equivalent test, the possibility of damage to the hollow insulator was low in the model with rupture disks, and the damage reduction effect of rupture disks is expected.

This analysis method is helpful for ground fault design on cable termination for high voltage and large capacity.

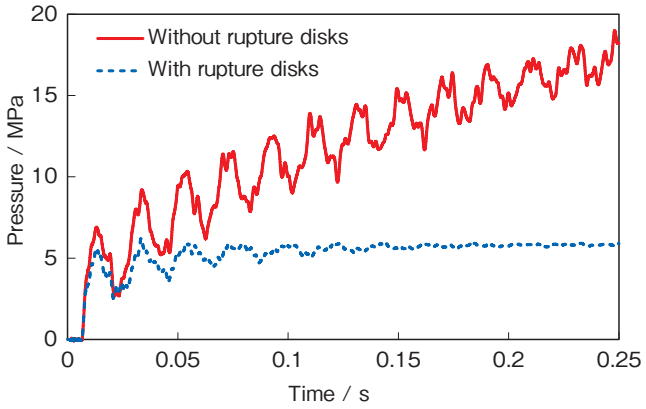

Figure 8 Simulation results of the internal pressure at ground fault in the 500 kV hollow insulator.

4. ANALYSIS OF STEEL WIRE ARMOUR LOSS IN SUBMARINE CABLE

Submarine power cables, which are used for offshore wind power generation, are also becoming higher in voltage and larger in capacity. Figure 9 shows a photograph of representative structure for three-core submarine power cables. A feature of submarine power cables is that they are provided with an armour layer on the outermost layer for the purposes of distributing installation tension to the seabed and preventing damage, and galvanized steel wires are usually used. This causes the following problems.

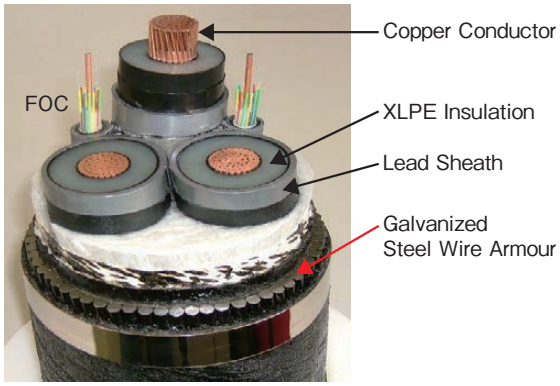

Figure 9 An example of a three-core submarine cable.

Power transmission is achieved by the current flowing through the conductor. At that time, the heat loss is generated inside the cable in operation, and an accurate estimation of these losses are very important in designing the size of an actual power cable. The reason is follows. In the actual cable size design, the conductor size is determined by constraining the maximum temperature (generally 90°C) of the cable conductor part in considering heat generation by ohmic loss in conductor and armour and dielectric loss, and heat dissipation in cable materials. Here, if the loss was over estimated, it leads to designing a larger size than necessary. In particular, submarine power cables use galvanized steel wires as the armour layer material, as mentioned above. Since steel wire is a magnetic material, it is induced by the electromagnetic field created by conductor currents, generating eddy currents and circuit currents, resulting in heat loss (called armour loss). The armour loss is generally calculated using the equation of the International Electrotechnical Commission (IEC) standard[5], but it has been qualitatively suggested that the larger the conductor and the larger the current, the more the armour loss is overestimated[6]. In other words, armour losses are possible to estimate more accurately, it will be possible to design a smaller size conductor than the conventional cable. With this in mind, accurately estimation for armour losses is being studied in our company[7] and the details are described below.

Finite element analysis (FEM analysis) was applied to evaluate the armour losses. Although it is possible to measure the current loss generated in the steel wire armour layer using an actual submarine cable, it takes time to prepare for the measurement and to evaluate the measurement. In contrast, analysis has the advantage of being able to evaluate losses and taking account of assigning all design parameters, and to derive results in a short period of time. The basic structure of the three-core submarine power cable which is the subject of this study consists of a power core, in which the conductor through which the current flows for power transmission is covered with an insulating layer, a lead sheath, and outer sheath. The three cores are twisted in the longitudinal direction, and the circumference is covered with the steel wire armour layer in the longitudinal direction. In addition, the phases of the AC currents flowing through the conductor of each of the three cores are shifted by 120 degrees, making the electromagnetic mechanism inside the cable extremely complex. Since the armour loss that is the object of this study is the loss that occurs as an electromagnetic element in this cable, it was considered that evaluation with finite element analysis would be useful.

For the FEM analysis, it was modeled as shown in Figure 10 since the only metal portions (copper conductor, lead sheath, steel wire armour layer) of the actual cable structure are affected by the electromagnetic field. Figure 10 shows also an example of the loss density distribution obtained when calculating with this model.

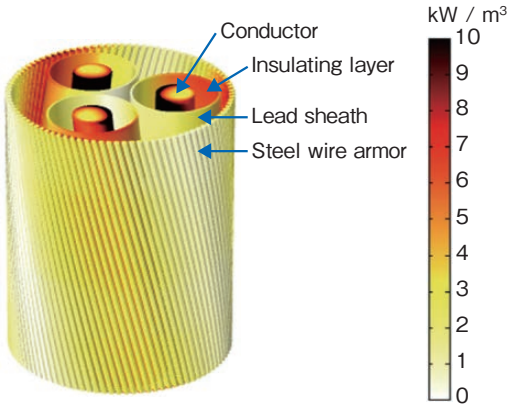

Figure 10 An example of loss density distribution in 3D FEM.

Using this model, the armour losses were evaluated when changing the conductor size, which is an important cable design parameter. And armour losses are expressed as λ_2 (armour loss rate: the ratio of armour losses to conductor loss) in the IEC standard, therefore it is also evaluated using λ_2 in this study. Figure 11 shows the change in λ_2 depending on the conductor size obtained by the analysis. Here, the value obtained by the IEC equation is indicated as λ_{2_IEC}, and the value obtained by analysis as λ_{2_FEM}. $\lambda_{2\_FEM}/\lambda_{2\_IEC}$ is also indicated as their ratio. As shown in the figure, λ_{2_FEM} has a smaller value than λ_{2_IEC} in any conductor sizes, and the ratio was about 60-70%, which was almost constant regardless of the conductor size.

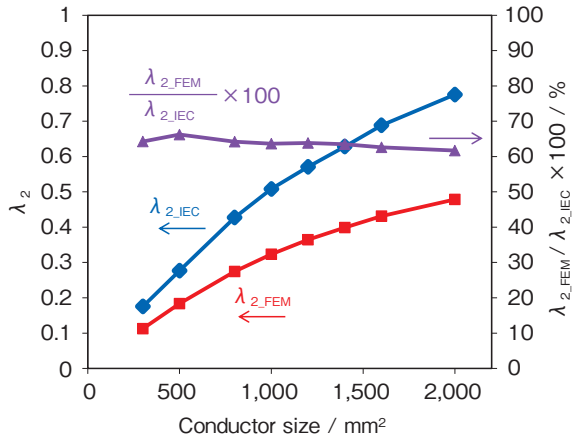

Figure 11 Comparison of the armour loss rate λ_2 between FEM analysis and IEC equation.

However, the larger the conductor size, the larger the difference in the calculated λ_2 value. Figure 12 shows the result of allowable current calculation using λ_{2_IEC} and λ_{2_FEM} for cases with a conductor size of 1,000 mm^2 or more. As shown in the figure, even in cases where a conductor size of 2,000 mm^2 is required when using λ_{2_IEC}, a conductor size of approximately 1,700 mm^2 can be designed using λ_{2_FEM}. That is, if the evaluation of λ_{2_IEC} is excessive, it can be said that a more compact cable design becomes feasible.

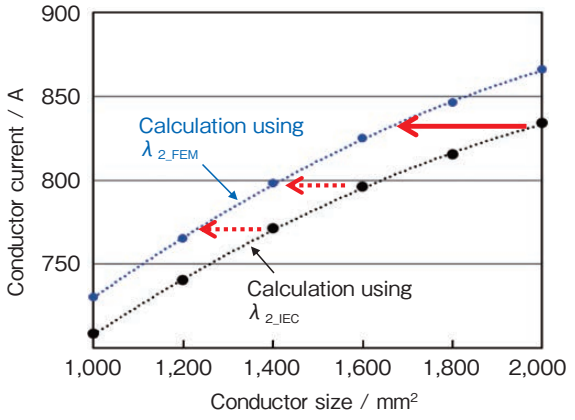

Figure 12 Difference of conductor designs depending on λ_{2_IEC} and λ_{2_FEM}.

And since armor losses are generated by magnetic fields, we considered that the influence of other metal materials should also be considered, and investigated the dependence of armour losses on lead sheath thickness by FEM analysis as well. Figure 13 shows the results. In this study, the conductor size was fixed at 1,400 mm^2, and only the lead sheath thickness was changed (275 kV 3x1,400 mm^2 submarine cable, outer diameter of ϕ280 mm approx.). In the figure, λ_{2_IEC} is a value based on the IEC equation, and since it focuses only on the armour layers, it is a constant value regardless of the lead thickness. On the other hand, λ_{2_FEM} showed a smaller value than λ_{2_IEC}, and there was a tendency for the value to decrease as the lead thickness increased. The reason for this result is considered to be the change in the electromagnetic field inside the cable and in the armour layers due to the change in the thickness of the lead sheath. In other words, the losses of armour layers are independent from the lead sheath thickness in the IEC equation, but it is indicated that the lead sheath layer influenced to armour losses by using FEM analysis.

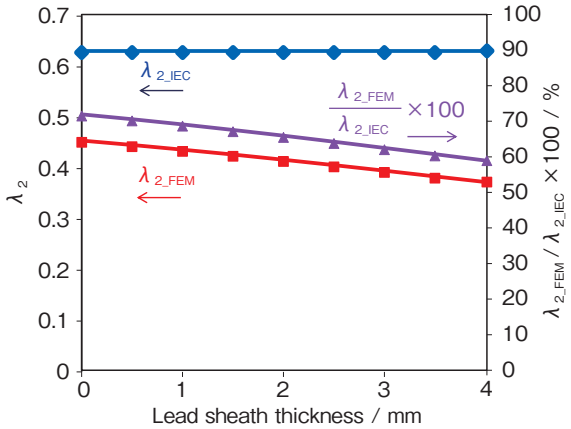

Figure 13 Dependence of λ_2 on the lead sheath thickness.

As described above, the results of FEM analysis have revealed that the armour losses coefficient based on the conventionally applied IEC equation may have been overestimated, and that the thickness of the metal sheath also has an effect to armour losses. By taking into these factors account, more accurate armour loss evaluation will be possible, which is expected to lead to cost reductions through optimal cable design.

The validity of the analysis results obtained here were confirmed by armour loss measurements using an actual three-core submarine cable, we will report details at a later date.

5. CONCLUSION

Examples of the application of scientific calculations to the design and development of power cable systems were introduced.

At present, the computer ability has become very high,

and it is possible to perform highly accurate electromagnetic field analysis and advanced simulations that were not possible a decade ago. It contributes to the development of cable systems in a wide range of fields from the material development at the molecular level to the analysis of explosive phenomena. In this way, by incorporating scientific calculations into the development of power cable systems, which has conventionally been performed on an experimental basis, it would be understood that have made product development more efficient.

Although not described in this paper, there are dedicated simulation software (for example, OrcaFlex) for dynamic analysis on marine systems in the marine field, and in Europe, they are generally adopted as tools for marine system design and are becoming standard. It is the reason why difficult to construct an experimental model due to the complexity of ocean phenomena, let alone actual-scale verification in the ocean. In offshore wind power research in Japan, marine system simulation software has begun to be applied to behavior analysis of cables connected to wind turbines and cable laying analysis.

Finally, in order to correctly understand the essence of issues, experiments with actual products will not disappear. However as industrial products become larger and more complex, product development using CAE or simulation technology will be essential. By combining them and promoting efficient product developments, we will achieve our 2025 mid-term plan, and also contribute to society by reducing costs and shortening the development period as well through technological development in the relevant field.

REFERENCES

1) T.Takada, T. Tohmine, Y. Tanaka, and J. Li: Space Charge Accumulation in Double-Layer Dielectric Systems – Measurement Methods and Quantum Chemical Calculations, IEEE EI Magazine, Vol. 35, No. 5 (2019), 36-46.
2) N. Shigemori, M. Yagi, and T. Tabuchi: Development of 350 kV and 525 kV HVDC extruded cable system, Jicable'19, (2019), A9-5.
3) Home page of Furukawa Electric > News release> Long-term load testing of DC 525kV class cable system completed. (Date of reference: December 14th, 2022) https://www.furukawa.co.jp/release/2021/ene_20210430.html (in Japanese)
4) Mark L.Wilkins: Computer simulation of dynamic phenomena, Springer, 2009.
5) IEC 60287-1-1, 2006, Electric cables-Calculation of the current rating-Part 1-1: Current rating equations (100% load factor) and calculation of losses-General.
6) J.J. Bremnes: "Power loss and inductance of steel armoured multi-core cables: comparison of IEC values with "2,5D" FEA results and measurements", Cigre 2010, 2020, B1-116.
7) Y. Matsumoto, et al., "3D FEM analysis of armour loss in three core submarine cables", Jicable'19, (2019), C8-1.